Clusters Containing Carbene Ligands. 13. Studies of the Reactivity of a Bridging Aminocarbene Center with Diarylalkynes in an Osmium Cluster Complex

Richard D. Adams* and Gong Chen

Department of Chemistry, University of South Carolina, Columbia, South Carolina 29208

Received March 21, 1991

From the reaction of $Os_3(CO)_9[\mu_3\text{-}C(Et)NMe(CH)](\mu\text{-}H)_2$ (1) with Me_3NO in $MeCN/CH_2Cl_2$ solution the lightly stabilized complex $Os_3(CO)_8(NCMe)[\mu_3\text{-}C(Et)NMe(CH)](\mu\text{-}H)_2$ (2) was obtained in 36% yield. Compound **2** reacts with PhC_2Ph or $TolC_2Tol$ at 68 °C to yield two isomers: $Os_3(CO)_8[\mu_3\text{-}\eta^2\text{-}C(H)N(Me)C(Et)][\eta^2\text{-}CArC(H)Ar](\mu\text{-}H)$ **3a,b**, 25%; **4a,b**, 13%; Ar = Ph, Tol). Compounds **3a,b** were isomerized to **4a,b** at 97 °C, but the reverse did not occur. At 97 °C compounds **4a,b** were isomerized further to $Os_3(CO)_8[\mu_3\text{-}ArC(H)CArCCN(Me)CEt](\mu\text{-}H)_2$ (**5a,b**) in 20% yield. When **5a,b** were treated with PMe_2Ph at 68 °C, the adducts $Os_3(CO)_8(PPhMe_2)[\mu_3\text{-}ArH_2CArCCN(Me)CEt](\mu\text{-}H)$ (**6a,b**; Ar = Ph, Tol) were obtained in 30–40% yield. Compounds **3a**, **4a**, **5b**, and **6a** were characterized crystallographically. Compounds **3a** and **4a** contain $\sigma\text{-}\pi$ diphenylvinyl ligands formed by insertion of the PhC_2Ph molecule into the metal–hydrogen bonds of the hydride ligands. They are positioned on different edges of the cluster in **3a** and **4a**. In compound **5b** the alkenyl ligand is coupled to the carbon atom that was formerly the bridging carbene ligand in **3a** and **4a**, and the hydrogen atom on that carbene carbon was shifted to the metal atoms. The addition of the PMe_2Ph ligand to **5a** resulted in a reductive elimination of a C–H bond to form a benzyl group in **6a**. Crystal data: For **3a**, space group = $P\bar{1}$, $a = 12.056$ (4) Å, $b = 14.229$ (4) Å, $c = 9.932$ (3) Å, $\alpha = 103.49$ (3)°, $\beta = 112.07$ (2)°, $\gamma = 65.68$ (2)°, $Z = 2$, 2777 reflections, R $c = P\bar{1}$, $a = 10.381$ (2) Å, $b = 16.410$ (3) Å, $c = 9.250$ (2) Å, $\alpha = 104.41$ (1)°, $\beta = 100.60$ (1)°, $\gamma = 73.91$ (1)°, $Z = 2$, 2898 reflections, $R = 0.039$; for **5b**, space group = $P\bar{1}$, $a = 10.401$ (2) Å, $b = 17.534$ (2) Å, $c = 9.979$ (2) Å, $\alpha = 92.31$ (1)°, $\beta = 116.15$ (1)°, $\gamma = 73.50$ (1)°, $Z = 2$, 3335 reflections, $R = 0.032$; for **6a**, space group = $P2/c$, $a = 12.740$ (4) Å, $b = 14.767$ (4) Å, $b = 14.767$ (4) Å, $c = 19.355$ (3) Å, $\beta = 98.12$ (2)°, $Z = 4$, 4261 reflections, $R = 0.022$.

Introduction

For many years metal complexes containing carbene ligands have been of interest because of their unusual structures and bonding.[1] Recently, these complexes have attracted attention as reagents for use in novel organic syntheses.[2] The study of carbene ligands in metal cluster complexes has been slow to develop due to the relative paucity of known examples.[3]

We have recently reported the preparation and structural characterization of the new compound $Os_3(CO)_9[\mu_3\text{-}HCN(Me)CEt](\mu\text{-}H)_2$ (1), which was obtained by a series of decarbonylations and CH activations of an *N*-methyl group on the ethyl(dimethylamino)carbene ligand in the complex $Os_3(CO)_{11}[C(Et)NMe_2]$.[4]

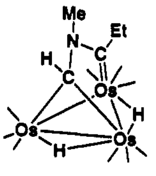

1

Compound 1 contains both bridging and terminal carbene centers. We were interested in trying to ascertain the differences in the reactivity of the two carbene centers. To do this we converted compound 1 into a more active form $Os_3(CO)_8(NCMe)[\mu_3\text{-}HCN(Me)CEt](\mu\text{-}H)_2$ (2) by treatment with Me_3NO in NCMe and then investigated the reactions of 2 with diarylalkynes. A pattern of insertion reactions involving the hydride ligands followed by coupling of the alkenyl groups to the bridging carbene center was observed. These results are reported here.

Experimental Section

General Methods. Although the reaction products are air stable, all of the reactions were performed under an atmosphere of nitrogen. $Os_3(CO)_9[\mu_3\text{-}C(Et)NMe(CH)](\mu\text{-}H)_2$ (1) was prepared by the previously reported procedure.[4] Diphenylacetylene and ditolylacetylene were purchased from Aldrich and were used without further purification. IR spectra were recorded on a Nicolet 5DXB FTIR spectrophotometer. ^1H NMR spectra were recorded on a Bruker AM-300 or AM-500 spectrometer operating at 300 or 500 MHz, respectively. Elemental analyses were performed by Desert Analytics, Tucson, AZ. TLC separations were performed in air on Whatman 0.25-mm silica gel 60-Å F_{254} plates.

Synthesis of Compound 2. A solution of Me_3NO (80 mg) in CH_3CN (10 mL) was added through a dropping funnel to a refluxing solution of 1 (212 mg, 0.234 mmol) in CH_2Cl_2 (80 mL) over a period of 20 min. After addition the solvent was removed in vacuo and the residue was separated by TLC on silica gel. Elution with a CH_2Cl_2/hexane (3/8) solvent mixture yielded 75.6 mg of yellow $Os_3(CO)_8(NCMe)[\mu_3\text{-}C(Et)NMe(CH)](\mu\text{-}H)_2$ (**2**, 36%). Spectral data for 2 are listed in Table I. Anal. Calcd for 2: C, 19.55; N, 3.04; H, 1.52. Found: C, 19.47; N, 2.91; H, 1.54.

Reaction of 2 with Diarylalkynes. (1) With PhC_2Ph. To a solution of 2 (20.0 mg, 0.0217 mmol) in hexane (50 mL) was added a solution of PhC_2Ph (20.0 mg) in hexane (20 mL). The solution mixture was refluxed for 20 min, and then the solvent was removed in vacuo. The residue was separated by TLC with a CH_2Cl_2/hexane (1/9) solvent mixture to yield 5.8 mg of yellow $Os_3(CO)_8[\mu_3\text{-}\eta^2\text{-}C(H)N(Me)C(Et)][\eta^2\text{-}C(Ph)C(H)Ph](\mu\text{-}H)$ (**3a**, 25%) and 3.0 mg of its orange isomer **4a** (13%). Anal. Calcd for **3a** and **4a**: C, 30.64; N, 1.32; H, 1.99. Found for **3a**: C, 30.43; N, 1.25; H, 1.74. Found for **4a**: C, 30.31; N, 1.34; H, 1.76.

(2) With $TolC_2Tol$. To a solution of 2 (41.3 mg, 0.0449 mmol) in hexane (50 mL) was added a solution of $TolC_2Tol$ (40 mg) in hexane (10 mL). The solution was refluxed for 15 min, and then

---

[1] Dötz, K. H.; Fischer, H.; Hofmann, P.; Kreissel, F. R.; Schubert, U.; Weiss, K. *Transition Metal Carbene Complexes*; Verlag Chemie: West Germany, 1983.

[2] (a) Collman, J. P.; Hegedus, L. S.; Norton, J. R.; Finke, R. G. *Principles and Applications of Organotransition Metal Chemistry*; University Science Books: Mill Valley, CA, 1987; Chapter 16. (b) Dötz, K. H. *Angew. Chem., Int. Ed. Engl.* **1984**, *23*, 587. (c) Dötz, K. H. *Pure Appl. Chem.* **1983**, *55*, 1689. (d) Semmelhack, M. F.; Bozell, J. J.; Sato, T.; Wulff, W.; Spiess, E.; Zask, A. *J. Am. Chem. Soc.* **1982**, *104*, 5850.

[3] Adams, R. D. *Chem. Rev.* **1989**, *89*, 1703.

[4] Adams, R. D.; Chen, G. *J. Cluster Sci.*, in press.

0276-7333/91/2310-3028$02.50/0 © 1991 American Chemical Society

Table I. IR and ^1H NMR Spectral Data for Compounds 2–6

compd	IR, $\nu(CO)$ cm^{-1} (in hexane)	^1H NMR, δ (in $CDCl_3$)
$Os_3(CO)_8(NCMe)[\mu_3\text{-}\eta^2\text{-}CHN(Me)C(Et)](\mu\text{-}H)_2$ (**2**)	2073 s, 2032 vs, 2018 vs, 1996 vs, 1970 m, 1959 s, 1943 s	6.13 (1 H, s, CH), 3.30 (3 H, s, NMe), 2.47 (1 H, dq, $^2J_{H-H}$ = 12.8 Hz, $^3J_{H-H}$ = 7.7 Hz, C*H*H), 2.36 (1 H, dq, $^2J_{H-H}$ = 12.8, $^3J_{H-H}$ = 7.7 Hz, CH*H*), 2.34 (3 H, s, NCMe), 0.86 (3 H, t, $^3J_{H-H}$ = 7.7 Hz, Me), −12.74 (1 H, s, OsH), −21.26 (1 H, s, OsH)
$Os_3(CO)_8[\mu_3\text{-}\eta^2\text{-}CHN(Me)C(Et)][\eta^2\text{-}C(Ph)C(H)Ph](\mu\text{-}H)$ (**3a**)	2062 s, 2051 s, 2017 vs, 2007 s, 1998 m, 1989 m, 1972 w, 1958 m	7.30–6.60 (10 H, m, Ph), 6.11 (1 H, s, CH), 3.45 (3 H, s, NMe), 2.88 (1 H, s, C=CH), 2.83 (1 H, dq, $^2J_{H-H}$ = 12.8 Hz, $^3J_{H-H}$ = 7.7 Hz, C*H*H), 2.73 (1 H, dq, $^2J_{H-H}$ = 12.8 Hz, $^3J_{H-H}$ = 7.7 Hz, CH*H*), 1.11 (3 H, t, $^3J_{H-H}$ = 7.7 Hz, Me), −12.92 (1 H, s, OsH)
$Os_3(CO)_8[\mu_3\text{-}\eta^2\text{-}CHN(Me)C(Et)][\eta^2\text{-}C(Tol)C(H)Tol](\mu\text{-}H)$ (**3b**)	2061 s, 2050 s, 2015 vs, 2006 vs, 1996 m, 1986 m, 1970 w, 1956 m	7.30–6.60 (8 H, m, Ph), 6.08 (1 H, s, CH), 3.43 (3 H, s, NMe), 2.86 (1 H, s, C=CH), 2.81 (1 H, dq, $^2J_{H-H}$ = 12.8 Hz, $^3J_{H-H}$ = 7.7 Hz, C*H*H), 2.71 (1 H, dq, $^2J_{H-H}$ = 12.8 Hz, $^3J_{H-H}$ = 7.7 Hz, CH*H*), 2.27 (3 H, s, Me(tol)), 2.21 (3 H, s, Me(tol)), 1.09 (3 H, t, $^3J_{H-H}$ = 7.7 Hz), −12.96 (1 H, s, OsH)
$Os_3(CO)_8[\mu_3\text{-}\eta^2\text{-}CHN(Me)C(Et)][\eta^2\text{-}C(Ph)C(H)Ph](\mu\text{-}H)$ (**4a**)	2063 m, 2044 s, 2013 vs, 1996 w, 1983 m, 1974 w, 1955 m	7.30–6.60 (10 H, m, Ph), 5.93 (1 H, s, CH), 3.57 (3 H, s, NMe), 3.10–2.90 (2 H, m, CH_2), 2.99 (1 H, s, C=CH), 1.16 (3 H, t, $^3J_{H-H}$ = 7.7 Hz, Me), −13.67 (1 H, s, OsH)
$Os_3(CO)_8[\mu_3\text{-}\eta^2\text{-}CHN(Me)C(Et)][\eta^2\text{-}C(Tol)C(H)Tol](\mu\text{-}H)$ (**4b**)	2062 m, 2043 s, 2012 vs, 1994 w, 1981 m, 1973 w, 1954 m	7.30–6.60 (8 H, m, Ph), 5.87 (1 H, s, CH), 3.55 (3 H, s, NMe), 3.10–2.90 (2 H, m, CH_2), 2.96 (1 H, s, C=CH), 2.27 (3 H, s, Me(tol)), 2.24 (3 H, s, Me(tol)), 1.15 (3 H, t, $^3J_{H-H}$ = 7.7 Hz, Me), −13.68 (1 H, s, OsH)
$Os_3(CO)_8[\mu_3\text{-}PhHC(Ph)CCN(Me)C(Et)](\mu\text{-}H)_2$ (**5a**)	2083 vs, 2047 vs, 2020 vs, 2009 vs, 1986 s, 1968 s, 1963 m	7.30–6.80 (10 H, m, Ph), 3.64 (1 H, d, $^3J_{H-H}$ = 2.6 Hz, C=CH), 2.79 (1 H, dq, $^2J_{H-H}$ = 12.7 Hz, $^3J_{H-H}$ = 7.4 Hz, C*H*H), 2.61 (3 H, s, NMe), 2.38 (1 H, dq, $^2J_{H-H}$ = 12.7 Hz, $^3J_{H-H}$ = 7.4 Hz, CH*H*), 0.98 (3 H, t, $^3J_{H-H}$ = 7.4 Hz, Me), −15.91 (1 H, s, OsH), −16.02 (1 H, d, $^3J_{H-H}$ = 2.6 Hz, OsH)
$Os_3(CO)_8[\mu_3\text{-}TolHC(Tol)CCN(Me)C(Et)](\mu\text{-}H)_2$ (**5b**)	2082 vs, 2046 vs, 2018 vs, 2008 s, 1985 s, 1967 s, 1962 m	7.30–6.80 (8 H, m, Ph), 3.64 (1 H, d, $^3J_{H-H}$ = 2.6 Hz, C=CH), 2.80 (1 H, dq, $^2J_{H-H}$ = 12.6 Hz, $^3J_{H-H}$ = 7.7 Hz, C*H*H), 2.62 (3 H, s, NMe), 2.37 (1 H, dq, $^2J_{H-H}$ = 12.6 Hz, $^3J_{H-H}$ = 7.7 Hz, CH*H*), 2.30 (3 H, s, Me(tol)), 2.21 (3 H, s, Me(tol)), 0.98 (3 H, t, $^3J_{H-H}$ = 7.7 Hz, Me), −15.90 (1 H, s, OsH), −16.02 (1 H, d, $^3J_{H-H}$ = 2.6 Hz, OsH)
$Os_3(CO)_8(PMe_2Ph)[\mu_3\text{-}PhH_2C(Ph)CCN(Me)C(Et)](\mu\text{-}H)$ (**6a**)	2064 s, 2026 vs, 1998 m, 1987 s, 1969 w, 1959 m, 1944 w	7.60–6.80 (10 H, m, Ph), 3.54 (1 H, d, $^2J_{H-H}$ = 14.5 Hz, C*H*HPh), 2.98 (1 H, d, $^2J_{H-H}$ = 14.5, CH*H*Ph), 2.79 (3 H, s, NMe), 2.67 (1 H, dq, $^2J_{H-H}$ = 12.6 Hz, $^3J_{H-H}$ = 7.7 Hz, C*H*H), 2.47 (1 H, dq, $^2J_{H-H}$ = 12.6 Hz, $^3J_{H-H}$ = 7.7 Hz, CH*H*), 2.15 (3 H, d, $^2J_{P-H}$ = 9.0 Hz, PMe), 1.99 (3 H, d, $^2J_{P-H}$ = 8.9 Hz, PMe), 1.09 (3 H, t, $^3J_{H-H}$ = 7.7 Hz, Me), −15.71 (1 H, s, br, OsH)
$Os_3(CO)_8(PMe_2Ph)[\mu_3\text{-}TolH_2C(Tol)CCN(Me)CEt](\mu\text{-}H)$ (**6b**)	2063 s, 2024 vs, 1997 m, 1985 s, 1967 w, 1958 m, 1942 w	7.60–6.70 (8 H, m, Ph), 3.49 (1 H, d, $^2J_{H-H}$ = 12.5 Hz, C*H*HPh), 2.90 (1 H, d, $^2J_{H-H}$ = 12.5, CH*H*Ph), 2.77 (3 H, s, NMe), 2.67 (1 H, dq, $^2J_{H-H}$ = 12.7 Hz, $^3J_{H-H}$ = 7.7 Hz, C*H*H), 2.46 (1 H, dq, $^2J_{H-H}$ = 12.9 Hz, $^3J_{H-H}$ = 7.7 Hz, CH*H*), 2.19 (3 H, s, Me(tol)), 2.15 (3 H, s, Me(tol)), 2.14 (3 H, d, $^2J_{P-H}$ = 9.2 Hz, PMe), 1.99 (3 H, d, $^2J_{P-H}$ = 8.8 Hz, PMe), 1.08 (3 H, t, $^3J_{H-H}$ = 7.7 Hz, Me), −15.66 (1 H, s, br, OsH)

the solvent was removed in vacuo. The residue was separated by TLC with CH_2Cl_2/hexane (2/8) solvent mixture to yield 12.3 mg of yellow $Os_3(CO)_8[\mu_3\text{-}\eta^2\text{-}C(H)N(Me)C(Et)][\eta^2\text{-}C(Tol)C(H)Tol](\mu\text{-}H)$ (**3b**, 25%) and 6.5 mg of its orange isomer **4b** (13%). Spectral data for **3a**, **3b**, **4a**, and **4b** are listed in Table I.

Thermolysis of 3a. A solution of **3a** (14.3 mg, 0.0135 mmol) in heptane (50 mL) was refluxed for 1 h. The solvent was then removed in vacuo, and the residue was separated by TLC. Elution with CH_2Cl_2/hexane (2/8) solvent mixture yielded 3.0 mg of orange **4a** (21%), 3.4 mg of yellow $Os_3(CO)_8[\mu_3\text{-}Ph(H)CPhCCN(Me)CEt](\mu\text{-}H)_2$ (**5a**, 23%), and 9.4 mg of unreacted **3a**.

Thermolysis of 3b. A solution of **3b** (20.0 mg, 0.0184 mmol) in heptane (20 mL) was refluxed for 50 min. The solvent was then removed in vacuo, and the residue was separated by TLC. Elution with CH_2Cl_2/hexane (1/9) yielded 3.3 mg of orange **4b** (17%), 5.2 mg of yellow $Os_3(CO)_8\{\mu_3\text{-}C[C(Tol)CH(Tol)]N(Me)C(Et)\}(\mu\text{-}H)_2$ (**5b**, 26%), and 5.5 mg of unreacted **3b**. Anal. Calcd for **5b**: C, 32.07; N, 1.29; H, 2.32. Found: C, 32.12; N, 1.17; H 2.22. Spectral data for **5a** and **5b** are listed in Table I.

Thermolysis of 4a. A solution of **4a** (11.0 mg, 0.0104 mmol) in heptane (20 mL) was refluxed for 1.5 h. The solvent was then removed in vacuo, and the residue was separated by TLC. Elution with CH_2Cl_2/hexane (1/9) solvent mixture yielded 1.0 mg of **5a** (9%) and 8.0 mg of unreacted **4a**. The remainder of the material was uncharacterizable decomposition.

Thermolysis of 4b. A solution of **4b** (12.2 mg, 0.0112 mmol) in heptane (20 mL) was refluxed for 1 h. The solvent was removed in vacuo, and the residue was separated by TLC. Elution with CH_2Cl_2/hexane (1/9) solvent mixture yielded 1.0 mg of **5b** (8%) and 7.8 mg of unreacted **4b**. The remainder of the material was uncharacterizable decomposition.

Reaction of 5a and 5b with $PPhMe_2$. To a solution of **5a** (29 mg, 0.027 mmol) in hexane (20 mL) was added 20 mL of PMe_2Ph. The solution was refluxed for 20 min, and then the solvent was removed in vacuo. Separation by TLC with CH_2Cl_2/hexane (1/4) solvent mixture yielded orange $Os_3(CO)_8(PMe_2Ph)[\mu_3\text{-}PhH_2C(Ph)CCN(Me)CEt](\mu\text{-}H)$ (**6a**; 9.4 mg, 29%), unreacted **5a** (4.7 mg), and few uncharacterizable trace products. Anal. Calcd for **6a**: C, 34.91; N, 1.16; H, 2.69. Found: C, 35.15; N, 1.15; H, 2.50. The reaction of **5b** with $PPhMe_2$ was performed similarly and yielded orange $Os_3(CO)_8(PPhMe_2)[\mu_3\text{-}TolH_2C(Tol)CCN(Me)CEt](\mu\text{-}H)$ (**6b**; 7.7 mg, 38%). Spectral data for **6a** and **6b** are listed in Table I.

Crystallographic Analyses. Crystals of **3a** suitable for X-ray diffraction analyses were grown from solution in hexane/CH_2Cl_2 solvent mixtures by slow evaporation of the solvent at 25 °C. Crystals of **4a** and **5b** were grown from a hexane/CH_2Cl_2 solvent mixture by slow evaporation of solvent at 0 °C. Crystals of **6a** were grown from a $MeOH/CH_2Cl_2$ solvent mixture by slow evaporation of solvent at 0 °C. All data crystals were mounted in thin-walled glass capillaries. Diffraction measurements were made on a Rigaku AFC6S automatic diffractometer by using graphite-monochromatized Mo $K\alpha$ radiation. Unit cells were determined from 15 randomly selected reflections obtained by using the AFC6 automatic search, center, index, and least-squares routines. Crystal data, data collection parameters, and results of the analyses are listed in Table II. All data processing was performed on a Digital Equipment Corp. VAXstation 3520 computer by using the TEXSAN structure solving program library (version 5.0) obtained from the Molecular Structure Corp., The

Table II. Crystallographic Data for Compounds 3a, 4a, 5b, and 6a

	compd			
	3a	**4a**	**5b**	**6a**
empirical formula	$Os_3O_8NC_{27}H_{21}$	$Os_3O_8NC_{27}H_{21}$	$Os_3O_8NC_{29}H_{25}$	$Os_3PO_8NC_{35}H_{32}\cdot{}^1/_4H_2O$
fw	1058.06	1058.06	1086.12	1200.71
cryst system	triclinic	triclinic	triclinic	monoclinic
lattice params				
a, Å	12.056 (4)	10.381 (2)	10.401 (2)	12.740 (4)
b, Å	14.229 (4)	16.410 (3)	17.534 (2)	14.767 (4)
c, Å	9.932 (3)	9.250 (2)	9.979 (2)	19.355 (3)
α, deg	103.49 (3)	104.41 (1)	92.31 (1)	
β, deg	112.07 (2)	100.60 (1)	116.15 (1)	98.12 (2)
γ, deg	65.68 (2)	73.91 (1)	73.50 (1)	
V, Å^3	1433 (2)	1455.3 (5)	1558.8 (4)	3605 (3)
space group	$P\bar{1}$ (No. 2)	$P\bar{1}$ (No. 2)	$P\bar{1}$ (No. 2)	$P2/c$ (No. 13)
Z	2	2	2	4
D_{calc}, g/cm^3	2.45	2.41	2.31	2.21
μ(Mo Kα), cm^{-1}	133.32	131.23	122.55	106.54
temp, °C	20	20	20	20
$2\theta_{max}$, deg	44.0	44.0	44.1	46.0
no. of observns ($I > 3\sigma(I)$)	2777	2898	3335	4261
no. of variables	352	355	382	447
residuals: R, R_w	0.026, 0.026	0.039, 0.049	0.032, 0.028	0.022, 0.025
goodness of fit indicator	1.17	2.27	1.62	1.35
max shift in final cycle	0.00	0.04	0.18	0.09
largest peak in final diff map, e/Å^3	1.16	1.29	0.47	0.66
abs corr (max/min)	empirical (1.00/0.73)	empirical (1.00/0.95)	empirical (1.00/0.69)	empirical (1.00/0.51)
scan speed, deg/min	4.0	4.0	4.0	4.0

Woodlands, TX. Neutral-atom scattering factors were calculated by the standard procedures.[5a] Anomalous dispersion corrections were applied to all non-hydrogen atoms.[5b] Full-matrix least-squares refinements minimized the function: $\Sigma_{hkl} w(|F_o| - |F_c|)^2$, where $w = 1/\sigma(F)^2$, $\sigma(F) = \sigma(F_o^2)/2F_o$, and $\sigma(F_o^2) = [\sigma(I_{raw})^2 + (0.02I_{net})^2]^{1/2}/Lp$.

Compounds **3a**, **4a**, and **5b** crystallized in the triclinic crystal system. The centrosymmetric space group $P\bar{1}$ was assumed and confirmed by the successful solution and refinement of each of the structures. All three structures were solved by combinations of direct methods and difference Fourier syntheses. The coordinates of the heavy atoms were obtained by direct methods (MITHRIL). All remaining non-hydrogen atoms were subsequently obtained from difference Fourier syntheses. All non-hydrogen atoms were refined with anisotropic thermal parameters. The positions of the hydrogen atoms were calculated by assuming idealized grometries. The hydride ligand and H(20) of compound **3a** were located in difference Fourier syntheses but could not be refined. The hydride ligand and H(20) of compound **4a** were located in a difference Fourier synthesis. The position of the hydride ligand was successfully refined. For **5b** the hydride ligands and H(20) were located by difference Fourier syntheses and both were satisfactorily refined. All other hydrogen atom positions were calculated by assuming idealized geometries. Their contributions were added to the structure factor calculations, but their positions were not refined.

Compound **6a** crystallized in the monoclinic crystal system. The space groups $P2/c$ or Pc were indicated by the systematic absences in the data. The former was chosen initially and confirmed by the successful solution and excellent refinement of the structure. The structure was solved by a combination of direct methods (MITHRIL) and difference Fourier syntheses. All of the non-hydrogen atoms were refined with anisotropic thermal parameters. The positions of hydrogen atoms on the ligands were calculated by assuming idealized geometries. The hydride ligand, H(1), and H(2) were satisfactorily refined. The scattering contributions of all other hydrogen atoms were added to the structure factor calculations, but their positions were not refined. In the final stages of refinement and single peak of significant size (approximately 2 e/Å^3) that was remote from the complex was observed in a difference Fourier synthesis. It was assigned as oxygen (presumably from a water moelcule of crystallization) and was satisfactorily refined to an occupancy of 0.25.

Results

From the reaction of 1 with Me_3NO in $MeCN/CH_2Cl_2$ solution the lightly stabilized complex $Os_3(CO)_8(NCMe)[\mu_3\text{-}HCN(Me)CEt](\mu\text{-}H)_2$ (**2**) was obtained in 36% yield. The ^1H NMR resonances at $\delta = 6.13$ ppm and $\delta = 2.34$ ppm are indicative of the hydrogen atom on the bridging carbene carbon atom and the methyl of the MeCN ligand and confirm that **2** is simply a MeCN-substituted derivative of 1. A preliminary structural analysis showed that the MeCN ligand is coordinated to the metal atom that is bonded to both of the bridging hydride ligands.[6] The molecule has no symmetry; thus, the hydrogen atoms on the CH_2 grouping are diastereotopic. This inequivalence is also observed in the ^1H NMR spectrum of **2**; see Table I.

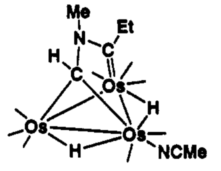

2

The reactions of **2** with PhC_2Ph and $TolC_2Tol$ have been investigated. Series of similar products were obtained for both reactions. From the reaction of **2** with PhC_2Ph at 68 °C two isomers were obtained: yellow $Os_3(CO)_8[\mu_3\text{-}\eta^2\text{-}C(H)N(Me)C(Et)][\eta^2\text{-}C(Ph)C(H)Ph](\mu\text{-}H)$ (**3a**, 25% yield) and orange isomer **4a** (13% yield). Both products were characterized by IR and ^1H NMR spectroscopy and by single-crystal X-ray diffraction analysis. ORTEP drawings of their molecular structures are shown in Figure 1 and 2. Final atomic positional parameters are listed in Tables III and IV. Selected interatomic distances and angles are listed in Tables V–VIII. Both molecules consist of triangular triosmium clusters bridged by the HCN(Me)CEt dicarbene ligand similar to that found in 1. The hydrogen-substituted carbon atom is a bridging carbene center. The ethyl-substituted carbon is a terminal carbene center.

---

(5) (a) *International Tables for X-ray Crystallograph*; Kynoch Press: Birmingham, England, 1975; Vol. IV, Table 2.2B, pp 99–101. (b) *Ibid.*, Table 2.3.1, pp 149–150.

(6) Crystal Data for 2: space group = $Pca2_1$, a = 15.58 (1) Å, b = 8.244 (3) Å, c = 32.95 (1) Å, Z = 8, 1628 reflections, R = 0.037.

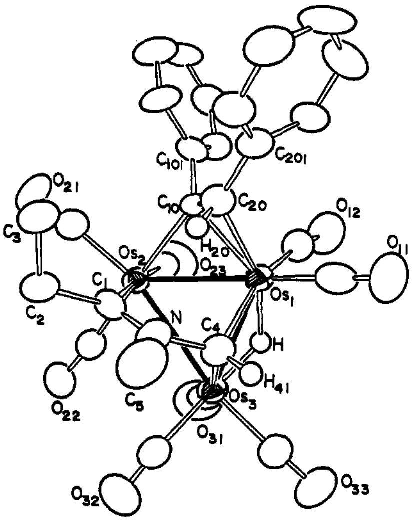

Figure 1. ORTEP diagram of $Os_3(CO)_8[\mu_3\text{-}\eta^2\text{-}C(H)N(Me)C(Et)][\eta^2\text{-}C(Ph)C(H)Ph](\mu\text{-}H)$ (**3a**), showing 50% probability thermal ellipsoids.

Table III. Positional Parameters and *B*(eq) Values for 3a

atom	*x*	*y*	*z*	*B*(eq), Å^2
Os(1)	0.63380 (04)	0.84208 (04)	0.33373 (05)	2.90 (2)
Os(2)	0.71605 (04)	0.62919 (03)	0.24168 (05)	2.65 (2)
Os(3)	0.46219 (04)	0.74963 (04)	0.28614 (05)	3.14 (3)
O(11)	0.5180 (10)	1.0743 (07)	0.3198 (11)	6.4 (6)
O(12)	0.7708 (09)	0.8758 (08)	0.6605 (10)	6.7 (6)
O(21)	0.9422 (08)	0.4679 (07)	0.1456 (10)	6.3 (6)
O(22)	0.5848 (08)	0.4722 (06)	0.1741 (09)	4.9 (5)
O(23)	0.8447 (09)	0.5805 (07)	0.5630 (09)	6.0 (6)
O(31)	0.5261 (10)	0.6158 (09)	0.5297 (10)	7.5 (8)
O(32)	0.2881 (09)	0.6514 (08)	0.0435 (10)	6.4 (7)
O(33)	0.2221 (10)	0.9133 (08)	0.3440 (12)	7.9 (7)
N	0.5131 (08)	0.7611 (07)	0.0123 (09)	3.4 (5)
C(1)	0.6099 (11)	0.6746 (09)	0.0289 (10)	3.0 (7)
C(2)	0.6463 (11)	0.6098 (10)	−0.1051 (13)	4.1 (7)
C(3)	0.7383 (12)	0.6397 (11)	−0.1400 (14)	5.3 (9)
C(4)	0.4790 (10)	0.8256 (08)	0.1369 (11)	3.3 (6)
C(5)	0.4311 (12)	0.8009 (11)	−0.1273 (13)	5.6 (8)
C(10)	0.8027 (09)	0.7462 (08)	0.2744 (10)	2.6 (5)
C(11)	0.5625 (12)	0.9837 (11)	0.3289 (13)	4.3 (8)
C(12)	0.7286 (11)	0.8564 (09)	0.5345 (14)	4.1 (7)
C(20)	0.7431 (10)	0.8296 (08)	0.1840 (12)	3.3 (6)
C(21)	0.8591 (11)	0.5286 (09)	0.1824 (12)	3.6 (7)
C(22)	0.6303 (11)	0.5345 (09)	0.2032 (12)	3.4 (7)
C(23)	0.7995 (11)	0.5989 (09)	0.4461 (14)	3.8 (7)
C(31)	0.5014 (11)	0.6685 (10)	0.4427 (13)	4.1 (7)
C(32)	0.3577 (12)	0.6846 (10)	0.1364 (14)	3.9 (7)
C(33)	0.3106 (12)	0.8510 (10)	0.3195 (14)	4.8 (8)
C(101)	0.9439 (10)	0.7196 (08)	0.3619 (12)	3.2 (6)
C(102)	0.9970 (11)	0.7108 (09)	0.5103 (13)	4.1 (7)
C(103)	1.1280 (12)	0.6807 (10)	0.5783 (14)	5.0 (8)
C(104)	1.2088 (12)	0.6564 (11)	0.5020 (19)	5.8 (9)
C(105)	1.1602 (13)	0.6621 (11)	0.3531 (19)	6 (1)
C(106)	1.0305 (11)	0.6939 (10)	0.2875 (14)	4.7 (8)
C(201)	0.8010 (10)	0.9040 (08)	0.1910 (12)	3.3 (6)
C(202)	0.8094 (12)	0.9180 (10)	0.0619 (14)	4.6 (8)
C(203)	0.8620 (13)	0.9849 (11)	0.0526 (15)	5.1 (9)
C(204)	0.9089 (12)	1.0423 (11)	0.1779 (18)	6 (1)
C(205)	0.9017 (12)	1.0305 (10)	0.3116 (16)	5.4 (8)
C(206)	0.8467 (11)	0.9637 (09)	0.3154 (13)	4.1 (7)

The dimensions of the dicarbene ligand are not significantly different in all three compounds.[4] Compounds **3a** and **4a** both contain a *cis*-diphenylvinyl group that is coordinated in the usual σ–π bridging coordination mode.[7] The complexes differ in the relative location of the diphenylvinyl group in the cluster. In **3a** it bridges the Os(1)–Os(2) bond, while in **4a** it bridges the Os(1)–Os(3) bond. Each isomer contains one hydride ligand. It bridges the Os(1)–Os(3) bond in **3a** and the Os(1)–Os(2) bond in **4a**. Two products **3b** and **4b** were obtained from the reaction of **2** with $TolC_2Tol$. The close similarity of their IR and ^1H NMR spectra to those of **3a** and **4a** indicates that they are a structurally analogous pair of isomers. We have found that **3a** can be isomerized to **4a** at 97 °C but not under the conditions of the original preparation, 68 °C. It thus appears that in the original reaction the isomers were formed by displacement of the MeCN ligand and the occurrence of two competing insertion reactions of the alkyne ligand into the metal–hydrogen bonds of each of the bridging hydride ligands of **2**.

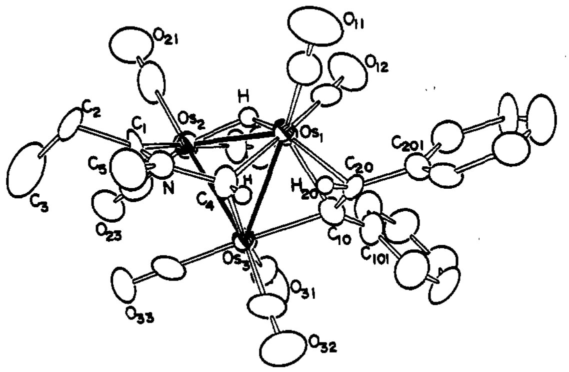

Figure 2. ORTEP diagram of $Os_3(CO)_8[\mu_3\text{-}\eta^2\text{-}C(H)N(Me)C(Et)][\eta^2\text{-}C(Ph)C(H)Ph](\mu\text{-}H)$ (**4a**), showing 50% probability thermal ellipsoids.

Table IV. Positional Parameters and *B*(eq) Values for 4a

atom	*x*	*y*	*z*	*B*(eq), Å^2
Os(1)	0.15140 (08)	0.82097 (05)	0.74177 (08)	2.65 (4)
Os(2)	0.03453 (08)	0.73144 (05)	0.46623 (08)	2.96 (4)
Os(3)	0.12133 (08)	0.66098 (05)	0.73986 (08)	2.42 (4)
O(11)	0.068 (02)	1.0139 (11)	0.877 (02)	8 (1)
O(12)	0.3847 (17)	0.8526 (12)	0.618 (02)	7 (1)
O(21)	−0.068 (02)	0.8238 (12)	0.208 (02)	7 (1)
O(22)	0.3254 (19)	0.6619 (13)	0.3743 (20)	7 (1)
O(23)	−0.0489 (16)	0.5735 (10)	0.2583 (16)	4.9 (9)
O(31)	0.3416 (16)	0.5008 (11)	0.6157 (19)	6 (1)
O(32)	0.1125 (18)	0.6169 (10)	1.0384 (19)	6 (1)
O(33)	−0.1055 (14)	0.5730 (10)	0.5865 (16)	4.6 (8)
N	−0.1449 (15)	0.8003 (09)	0.7066 (18)	2.9 (8)
C(1)	−0.1475 (17)	0.7798 (12)	0.560 (02)	3 (1)
C(2)	−0.290 (02)	0.8017 (14)	0.469 (02)	4 (1)
C(3)	−0.354 (03)	0.7266 (19)	0.416 (03)	8 (2)
C(4)	−0.0162 (19)	0.7876 (13)	0.800 (02)	4 (1)
C(5)	−0.261 (02)	0.8361 (14)	0.790 (03)	5 (1)
C(10)	0.2743 (19)	0.7269 (12)	0.867 (02)	3 (1)
C(11)	0.100 (02)	0.9424 (16)	0.829 (02)	4 (1)
C(12)	0.301 (02)	0.8385 (13)	0.666 (02)	4 (1)
C(20)	0.2294 (17)	0.8068 (12)	0.980 (02)	3 (1)
C(21)	−0.029 (02)	0.7890 (19)	0.306 (02)	5 (2)
C(22)	0.221 (02)	0.6884 (15)	0.413 (02)	4 (1)
C(23)	−0.019 (02)	0.6311 (15)	0.339 (02)	4 (1)
C(31)	0.261 (02)	0.5593 (15)	0.663 (02)	4 (1)
C(32)	0.118 (02)	0.6307 (12)	0.922 (02)	4 (1)
C(33)	−0.0226 (20)	0.6077 (11)	0.646 (02)	3 (1)
C(101)	0.4186 (20)	0.6787 (13)	0.872 (02)	3 (1)
C(102)	0.4938 (20)	0.6557 (15)	0.745 (02)	4 (1)
C(103)	0.623 (02)	0.6108 (15)	0.759 (02)	5 (1)
C(104)	0.687 (03)	0.5836 (15)	0.891 (03)	6 (1)
C(105)	0.616 (03)	0.6035 (19)	1.007 (03)	6 (2)
C(106)	0.483 (02)	0.6514 (15)	1.003 (02)	5 (1)
C(201)	0.3239 (18)	0.8563 (11)	1.080 (02)	3 (1)
C(202)	0.434 (02)	0.8708 (15)	1.034 (02)	5 (1)
C(203)	0.5103 (20)	0.9229 (17)	1.141 (03)	5 (1)
C(204)	0.477 (03)	0.9627 (19)	1.276 (03)	8 (2)
C(205)	0.362 (03)	0.9517 (15)	1.320 (03)	5 (1)
C(206)	0.284 (02)	0.8959 (12)	1.222 (02)	5 (1)

---

(7) Deeming, A. J. *Adv. Organomet. Chem.* **1986**, *26*, 1. (b) Clauss, A. D.; Tachikawa, M.; Shapley, J. R.; Pierpont, C. G. *Inorg. Chem.* **1981**, *20*, 1528.

Table V. Intramolecular Distances for 3a[a]

Os(1)-H	1.56	Os(3)-C(32)	1.89 (1)
Os(1)-C(11)	1.84 (1)	Os(3)-C(33)	1.89 (1)
Os(1)-C(12)	1.90 (1)	Os(3)-C(31)	1.95 (1)
Os(1)-C(10)	2.14 (1)	Os(3)-C(4)	2.14 (1)
Os(1)-C(4)	2.18 (1)	N-C(1)	1.29 (1)
Os(1)-C(20)	2.27 (1)	N-C(4)	1.44 (1)
Os(1)-Os(3)	2.730 (1)	N-C(5)	1.45 (1)
Os(1)-Os(2)	2.813 (1)	C(1)-C(2)	1.53 (1)
Os(2)-C(22)	1.91 (1)	C(2)-C(3)	1.51 (2)
Os(2)-C(21)	1.93 (1)	C(10)-C(20)	1.43 (1)
Os(2)-C(23)	1.96 (1)	C(10)-C(101)	1.52 (1)
Os(2)-C(1)	2.11 (1)	C(20)-C(201)	1.47 (1)
Os(2)-C(10)	2.21 (1)	O-C(av)	1.15 (1)
Os(2)-Os(3)	2.973 (1)	C-C(Ph)	1.38 (2)
Os(3)-H	1.48		

[a] Distances are in angstroms. Estimated standard deviations in the least significant figure are given in parentheses.

Table VI. Intramolecular Distances for 4a[a]

Os(1)-H	1.5 (1)	Os(3)-C(32)	1.88 (2)
Os(1)-C(11)	1.92 (2)	Os(3)-C(33)	1.90 (2)
Os(1)-C(12)	1.93 (3)	Os(3)-C(31)	1.96 (2)
Os(1)-C(10)	2.15 (2)	Os(3)-C(10)	2.17 (2)
Os(1)-C(4)	2.15 (2)	Os(3)-C(4)	2.18 (2)
Os(1)-C(20)	2.25 (2)	N-C(1)	1.31 (2)
Os(1)-Os(3)	2.724 (1)	N-C(4)	1.44 (2)
Os(1)-Os(2)	2.849 (1)	N-C(5)	1.46 (2)
Os(2)-H	1.7 (1)	C(1)-C(2)	1.56 (3)
Os(2)-C(21)	1.87 (3)	C(2)-C(3)	1.49 (4)
Os(2)-C(23)	1.93 (2)	C(10)-C(20)	1.48 (2)
Os(2)-C(22)	1.98 (2)	C(10)-C(101)	1.49 (3)
Os(2)-C(1)	2.09 (2)	O-C(av)	1.14 (2)
Os(2)-Os(3)	2.932 (1)	C(Ph)-C(av)	1.40 (3)

[a] Distances are in angstroms. Estimated standard deviations in the least significant figure are given in parentheses.

Table VII. Intramolecular Bond Angles for 3a[a]

C(11)-Os(1)-C(10)	123.7 (4)	C(1)-Os(2)-C(10)	87.4 (4)
C(11)-Os(1)-C(4)	89.8 (5)	C(1)-Os(2)-Os(1)	85.7 (3)
C(11)-Os(1)-C(20)	90.3 (4)	C(1)-Os(2)-Os(3)	81.4 (3)
C(11)-Os(1)-Os(3)	114.5 (4)	C(10)-Os(2)-Os(1)	48.7 (2)
C(11)-Os(1)-Os(2)	161.1 (4)	C(10)-Os(2)-Os(3)	104.6 (2)
C(12)-Os(1)-C(10)	92.9 (4)	Os(1)-Os(2)-Os(3)	56.22 (3)
C(12)-Os(1)-C(4)	160.3 (4)	C(32)-Os(3)-C(4)	93.2 (5)
C(12)-Os(1)-C(20)	112.7 (4)	C(32)-Os(3)-Os(1)	142.0 (3)
C(12)-Os(1)-Os(3)	112.4 (4)	C(32)-Os(3)-Os(2)	101.1 (3)
C(12)-Os(1)-Os(2)	106.8 (4)	C(33)-Os(3)-C(4)	98.9 (5)
C(10)-Os(1)-C(4)	103.0 (4)	C(33)-Os(3)-Os(1)	109.0 (4)
C(10)-Os(1)-C(20)	37.7 (4)	C(33)-Os(3)-Os(2)	167.8 (4)
C(10)-Os(1)-Os(3)	115.4 (3)	C(31)-Os(3)-C(4)	163.2 (4)
C(10)-Os(1)-Os(2)	50.9 (3)	C(31)-Os(3)-Os(1)	114.1 (3)
C(4)-Os(1)-C(20)	87.0 (4)	C(31)-Os(3)-Os(2)	92.5 (3)
C(4)-Os(1)-Os(3)	50.0 (3)	C(4)-Os(3)-Os(1)	51.6 (3)
C(4)-Os(1)-Os(2)	75.5 (3)	C(4)-Os(3)-Os(2)	72.6 (3)
C(20)-Os(1)-Os(3)	127.3 (3)	Os(1)-Os(3)-Os(2)	58.91 (3)
C(20)-Os(1)-Os(2)	77.3 (3)	C(1)-N-C(4)	120.8 (9)
Os(3)-Os(1)-Os(2)	64.87 (3)	C(1)-N-C(5)	124 (1)
C(22)-Os(2)-C(1)	88.8 (4)	C(4)-N-C(5)	115 (1)
C(22)-Os(2)-C(10)	175.7 (4)	N-C(1)-C(2)	119 (1)
C(22)-Os(2)-Os(1)	129.0 (3)	N-C(1)-Os(2)	118.5 (7)
C(22)-Os(2)-Os(3)	72.8 (3)	C(2)-C(1)-Os(2)	122.0 (8)
C(21)-Os(2)-C(1)	92.9 (4)	C(3)-C(2)-C(1)	112 (1)
C(21)-Os(2)-C(10)	87.9 (4)	N-C(4)-Os(3)	116.0 (7)
C(21)-Os(2)-Os(1)	136.6 (3)	N-C(4)-Os(1)	118.0 (7)
C(21)-Os(2)-Os(3)	165.9 (3)	Os(3)-C(4)-Os(1)	78.4 (4)
C(23)-Os(2)-C(1)	173.8 (5)	C(20)-C(10)-Os(1)	75.8 (6)
C(23)-Os(2)-C(10)	92.3 (4)	C(20)-C(10)-Os(2)	121.4 (7)
C(23)-Os(2)-Os(1)	89.4 (3)	Os(1)-C(10)-Os(2)	80.4 (3)
C(23)-Os(2)-Os(3)	92.6 (3)	Os-C(av)-O	176 (1)

[a] Angles are in degrees. Estimated standard deviations in the least significant figure are given in parentheses.

Additional isomers $Os_3(CO)_8[\mu_3\text{-ArC(H)CArCCN(Me)CEt}](\mu\text{-}H)_2$ (**5a,b**) (Ar = Ph, Tol (20% yield)) were also formed when **3a,b** was isomerized at 97 °C. Compounds **5a,b** were also formed by heating **4a,b** to 97 °C, but no isomerization to the compounds **3a,b** was observed in this reaction. Crystals of **5a** suitable for x-ray diffraction analyses could not be obtained, but suitable crystals of **5b** were obtained. An ORTEP drawing of the molecular structure of **5b** is shown in Figure 3. Final atomic positional parameters are listed in Table IX. Selected interatomic distances and angles are listed in Tables X and XI. The molecule consists of a triangular cluster of three osmium atoms with eight terminal carbonyl ligands and two bridging hydride ligands (located) and a EtCN(Me)CC(Tol)C(Tol) grouping. C(1) is a carbene center analogous to those found in the complexes **1**, **3a**, and **4a**. C(4) could be viewed as a bridging carbene as in **1**, **3a**, and **4a**, but since it is bonded to atoms C(10) and C(20), which are also metal coordinated, the entire C(4), C(10), C(20) grouping could be described better as an allyl group

Table VIII. Intramolecular Bond Angles for 4a[a]

Os(2)-Os(1)-Os(3)	63.44 (3)	Os(1)-Os(3)-Os(2)	60.35 (3)
Os(2)-Os(1)-C(4)	75.0 (5)	Os(1)-Os(3)-C(4)	50.6 (5)
Os(2)-Os(1)-C(10)	108.5 (5)	Os(1)-Os(3)-C(10)	50.6 (5)
Os(2)-Os(1)-C(11)	127.2 (6)	Os(1)-Os(3)-C(31)	118.2 (6)
Os(2)-Os(1)-C(12)	97.8 (6)	Os(1)-Os(3)-C(32)	119.9 (6)
Os(2)-Os(1)-C(20)	141.0 (4)	Os(1)-Os(3)-C(33)	129.7 (6)
Os(3)-Os(1)-C(4)	51.4 (6)	Os(2)-Os(3)-C(4)	72.9 (5)
Os(3)-Os(1)-C(10)	51.3 (5)	Os(2)-Os(3)-C(10)	105.0 (5)
Os(3)-Os(1)-C(11)	145.2 (6)	Os(2)-Os(3)-C(31)	98.4 (6)
Os(3)-Os(1)-C(12)	123.1 (6)	Os(2)-Os(3)-C(32)	161.5 (7)
Os(3)-Os(1)-C(20)	77.6 (4)	Os(2)-Os(3)-C(33)	78.2 (6)
C(4)-Os(1)-C(10)	84.9 (7)	C(4)-Os(3)-C(10)	83.8 (7)
C(4)-Os(1)-C(11)	96.4 (8)	C(4)-Os(3)-C(31)	168.1 (8)
C(4)-Os(1)-C(12)	172.3 (8)	C(4)-Os(3)-C(32)	93.1 (8)
C(4)-Os(1)-C(20)	79.9 (7)	C(4)-Os(3)-C(33)	92.6 (7)
C(10)-Os(1)-C(11)	122.7 (8)	C(10)-Os(3)-C(31)	90.9 (8)
C(10)-Os(1)-C(12)	95.0 (8)	C(10)-Os(3)-C(32)	84.8 (8)
C(10)-Os(1)-C(20)	39.1 (6)	C(10)-Os(3)-C(33)	174.1 (7)
C(11)-Os(1)-C(20)	84.5 (8)	C(1)-N-C(4)	119 (2)
C(12)-Os(1)-C(20)	104.8 (8)	C(1)-N-C(5)	126 (2)
Os(1)-Os(2)-Os(3)	56.21 (3)	C(4)-N-C(5)	114 (2)
Os(1)-Os(2)-C(1)	85.6 (5)	Os(2)-C(1)-N	119 (1)
Os(1)-Os(2)-C(21)	118.7 (7)	Os(2)-C(1)-C(2)	125 (1)
Os(1)-Os(2)-C(22)	85.5 (5)	N-C(1)-C(2)	115 (2)
Os(1)-Os(2)-C(23)	152.7 (6)	C(1)-C(2)-C(3)	114 (2)
Os(3)-Os(2)-C(1)	81.9 (6)	Os(1)-C(4)-Os(3)	78.0 (6)
Os(3)-Os(2)-C(21)	173.2 (8)	Os(1)-C(4)-N	120 (1)
Os(3)-Os(2)-C(22)	89.9 (6)	Os(3)-C(4)-N	115 (1)
Os(3)-Os(2)-C(23)	96.7 (6)	Os(1)-C(10)-Os(3)	78.2 (6)
C(1)-Os(2)-C(21)	94 (1)	Os(1)-C(20)-C(10)	67 (1)
C(1)-Os(2)-C(22)	170.3 (8)	Os-C(av)-O	177 (2)
C(1)-Os(2)-C(23)	93.7 (8)		

[a] Angles are in degrees. Estimated standard deviations in the least significant figure are given in parentheses.

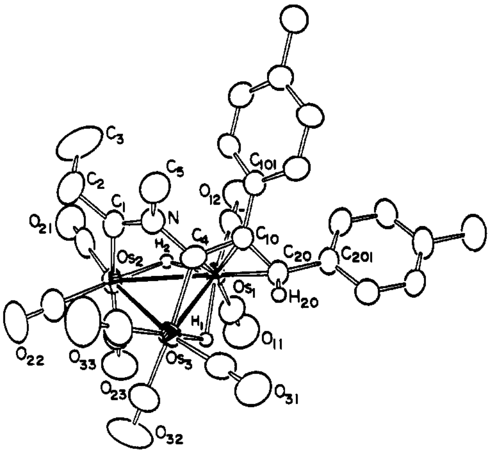

Figure 3. ORTEP diagram of $Os_3(CO)_8[\mu_3\text{-TolC(H)CTolCCN(Me)CEt}](\mu\text{-}H)_2$ (**5b**), showing 50% probability thermal ellipsoids.

Table IX. Positional Parameters and *B*(eq) Values for 5b[a]

atom	*x*	*y*	*z*	*B*(eq), Å^2
Os(1)	0.11176 (04)	0.201094 (19)	0.54192 (04)	2.62 (2)
Os(2)	0.05687 (04)	0.10124 (02)	0.28753 (04)	3.08 (2)
Os(3)	−0.13225 (04)	0.26001 (02)	0.25034 (04)	2.85 (2)
O(11)	0.0056 (10)	0.1433 (05)	0.7451 (09)	7.4 (6)
O(12)	0.4269 (08)	0.1317 (04)	0.7845 (09)	6.1 (4)
O(21)	0.2943 (09)	−0.0619 (04)	0.3730 (09)	6.4 (5)
O(22)	−0.1282 (09)	0.0827 (04)	−0.0415 (08)	6.6 (5)
O(23)	−0.1584 (09)	0.0471 (05)	0.3701 (09)	6.3 (5)
O(31)	−0.2983 (08)	0.4348 (04)	0.2494 (08)	5.7 (4)
O(32)	−0.4103 (09)	0.2037 (05)	0.1628 (11)	7.8 (5)
O(33)	−0.1714 (11)	0.2772 (05)	−0.0699 (09)	7.8 (6)
N	0.1725 (08)	0.2333 (04)	0.2573 (08)	3.1 (4)
C(1)	0.1780 (10)	0.1587 (05)	0.2260 (09)	3.5 (5)
C(2)	0.2589 (13)	0.1245 (06)	0.1352 (12)	5.3 (7)
C(3)	0.4213 (17)	0.0824 (08)	0.2365 (20)	9 (1)
C(4)	0.0907 (09)	0.2689 (05)	0.3440 (09)	2.9 (4)
C(5)	0.2154 (12)	0.2887 (06)	0.1865 (11)	4.4 (6)
C(10)	0.1656 (09)	0.3052 (04)	0.4736 (09)	2.6 (4)
C(11)	0.0479 (11)	0.1651 (06)	0.6677 (11)	4.3 (6)
C(12)	0.3083 (12)	0.1600 (06)	0.6920 (10)	3.9 (5)
C(20)	0.0896 (10)	0.3293 (05)	0.5665 (10)	3.0 (5)
C(21)	0.2067 (12)	−0.0011 (06)	0.3398 (10)	4.0 (6)
C(22)	−0.0563 (12)	0.0910 (06)	0.0829 (12)	4.4 (6)
C(23)	−0.0774 (12)	0.0656 (06)	0.3407 (11)	4.4 (6)
C(31)	−0.2311 (10)	0.3686 (06)	0.2518 (10)	3.7 (5)
C(32)	−0.3079 (12)	0.2249 (06)	0.1937 (11)	4.5 (6)
C(33)	−0.1597 (12)	0.2714 (06)	0.0509 (12)	4.7 (6)
C(101)	0.3166 (09)	0.3137 (05)	0.5161 (09)	2.9 (4)
C(102)	0.4429 (10)	0.2519 (05)	0.5343 (10)	3.4 (5)
C(103)	0.5763 (10)	0.2673 (05)	0.5648 (10)	3.6 (5)
C(104)	0.5894 (10)	0.3438 (05)	0.5798 (10)	3.3 (5)
C(105)	0.4630 (09)	0.4063 (05)	0.5659 (10)	3.2 (5)
C(106)	0.3311 (10)	0.3911 (05)	0.5361 (10)	3.4 (5)
C(107)	0.7319 (11)	0.3612 (06)	0.6083 (10)	3.9 (5)
C(201)	0.1477 (10)	0.3675 (05)	0.7087 (09)	2.9 (4)
C(202)	0.2923 (11)	0.3404 (05)	0.8245 (11)	4.2 (5)
C(203)	0.3377 (11)	0.3806 (06)	0.9499 (11)	4.3 (5)
C(204)	0.2427 (12)	0.4462 (06)	0.9700 (11)	4.2 (6)
C(205)	0.0984 (12)	0.4735 (06)	0.8581 (13)	4.7 (6)
C(206)	0.0518 (10)	0.4346 (05)	0.7284 (11)	4.0 (5)
C(207)	0.2944 (14)	0.4901 (07)	1.1103 (13)	6.7 (8)

Table X. Intramolecular Distances for 5b[a]

Os(1)–Os(2)	2.9612 (7)	Os(3)–C(31)	1.89 (1)
Os(1)–Os(3)	2.8667 (8)	Os(3)–C(32)	1.93 (1)
Os(1)–H(1)	1.91 (6)	Os(3)–C(33)	1.89 (1)
Os(1)–C(4)	2.241 (8)	Os(3)–H(1)	1.72 (6)
Os(1)–C(10)	2.265 (8)	N–C(1)	1.32 (1)
Os(1)–C(11)	1.86 (1)	N–C(4)	1.47 (1)
Os(1)–C(12)	1.87 (1)	N–C(5)	1.49 (1)
Os(1)–C(20)	2.208 (8)	C(1)–C(2)	1.49 (1)
Os(1)–H(2)	1.68 (8)	C(2)–C(3)	1.51 (2)
Os(2)–Os(3)	2.8436 (7)	C(4)–C(10)	1.42 (1)
Os(2)–C(1)	2.11 (1)	C(10)–C(20)	1.45 (1)
Os(2)–C(21)	1.92 (1)	C(10)–C(101)	1.49 (1)
Os(2)–C(22)	1.89 (1)	C(20)–C(201)	1.49 (1)
Os(2)–C(23)	1.95 (1)	C(20)–H(20)	0.80 (7)
Os(2)–H(2)	1.87 (8)	O–C(av)	1.15 (1)
Os(3)–C(4)	2.135 (8)	C–C(Ph)	1.38 (1)

[a] Distances are in angstroms. Estimated standard deviations in the least significant figure are given in parentheses.

Table XI. Intramolecular Bond Angles for 5b[a]

Os(2)–Os(1)–Os(3)	58.38 (2)	Os(2)–Os(3)–C(4)	74.3 (2)
Os(2)–Os(1)–C(4)	70.5 (2)	Os(2)–Os(3)–C(31)	170.8 (3)
Os(2)–Os(1)–C(10)	105.3 (2)	Os(2)–Os(3)–C(32)	92.7 (3)
Os(2)–Os(1)–C(11)	107.7 (3)	Os(2)–Os(3)–C(33)	89.7 (3)
Os(2)–Os(1)–C(12)	110.2 (3)	C(4)–Os(3)–C(31)	97.5 (3)
Os(2)–Os(1)–C(20)	135.0 (2)	C(4)–Os(3)–C(32)	165.2 (3)
Os(3)–Os(1)–C(4)	47.5 (2)	C(4)–Os(3)–C(33)	93.1 (4)
Os(3)–Os(1)–C(10)	76.7 (2)	C(1)–N–C(4)	117.3 (7)
Os(3)–Os(1)–C(11)	111.3 (3)	C(1)–N–C(5)	124.6 (7)
Os(3)–Os(1)–C(12)	159.6 (3)	C(4)–N–C(5)	116.9 (7)
Os(3)–Os(1)–C(20)	83.3 (2)	Os(2)–C(1)–N	118.7 (6)
C(4)–Os(1)–C(10)	36.7 (3)	Os(2)–C(1)–C(2)	124.7 (7)
C(4)–Os(1)–C(11)	157.1 (4)	N–C(1)–C(2)	116.3 (8)
C(4)–Os(1)–C(12)	114.4 (4)	C(1)–C(2)–C(3)	110 (1)
C(4)–Os(1)–C(20)	66.1 (3)	Os(1)–C(4)–Os(3)	81.8 (3)
C(10)–Os(1)–C(11)	144.9 (4)	Os(1)–C(4)–N	122.2 (5)
C(10)–Os(1)–C(12)	91.8 (3)	Os(1)–C(4)–C(10)	72.6 (5)
C(10)–Os(1)–C(20)	37.7 (3)	Os(3)–C(4)–N	113.6 (6)
C(11)–Os(1)–C(20)	107.7 (4)	Os(3)–C(4)–C(10)	128.7 (6)
C(12)–Os(1)–C(20)	97.9 (4)	N–C(4)–C(10)	117.7 (7)
Os(1)–Os(2)–Os(3)	59.15 (2)	Os(1)–C(10)–C(4)	70.7 (4)
Os(1)–Os(2)–C(1)	86.3 (2)	Os(1)–C(10)–C(20)	69.0 (5)
Os(1)–Os(2)–C(21)	112.4 (3)	Os(1)–C(10)–C(101)	127.3 (5)
Os(1)–Os(2)–C(22)	149.1 (3)	C(4)–C(10)–C(20)	115.7 (7)
Os(1)–Os(2)–C(23)	88.9 (3)	C(4)–C(10)–C(101)	122.2 (7)
Os(3)–Os(2)–C(1)	82.8 (2)	C(20)–C(10)–C(101)	122.0 (7)
Os(3)–Os(2)–C(21)	171.1 (3)	Os(1)–C(20)–C(10)	73.3 (5)
Os(3)–Os(2)–C(22)	90.0 (3)	Os(1)–C(20)–C(201)	127.4 (6)
Os(3)–Os(2)–C(23)	87.7 (3)	Os(1)–C(20)–H(20)	115 (5)
C(1)–Os(2)–C(21)	94.2 (4)	C(10)–C(20)–C(201)	125.1 (8)
C(1)–Os(2)–C(22)	88.8 (4)	C(10)–C(20)–H(20)	103 (5)
C(1)–Os(2)–C(23)	170.6 (4)	C(201)–C(20)–H(20)	108 (5)
Os(1)–Os(3)–Os(2)	62.47 (2)	Os(3)–H(1)–Os(1)	104 (3)
Os(1)–Os(3)–C(4)	50.7 (2)	Os(1)–H(2)–Os(2)	113 (4)
Os(1)–Os(3)–C(31)	109.2 (3)	Os–C(av)–O	177 (1)
Os(1)–Os(3)–C(32)	117.2 (3)	C(Ph)–C(av)–C	120 (1)
Os(1)–Os(3)–C(33)	137.6 (3)		

[a] Angles are in degrees. Estimated standard deviations in the least significant figure are given in parentheses.

metalated at C(4) and σ-bonded to Os(3) with all three carbon atoms π-bonded to Os(1), Os(1)–C(4) = 2.241 (8) Å, Os(1)–C(10) = 2.265 (8) Å, and Os(1)–C(20) = 2.208 (8) Å. The tolyl groups on C(10) and C(20) exhibit the cis stereochemistry as observed for the alkenyl groups in **3a** and **4a**. The hydride ligands bridge the Os(1)–Os(2) and Os(1)–Os(3) metal–metal bonds as in **1**. They exhibit separate resonances in the ^{1}H NMR spectrum, δ = −15.90 (s) and −16.02 ppm (d, $^2J_{HH}$ = 2.6 Hz). The latter shows a weak coupling to the hydrogen atom on C(20).

When **5a,b** were treated with PMe$_2$Ph in hexane at 68 °C, the adducts $Os_3(CO)_8(PMe_2Ph)[\mu_3\text{-}ArH_2CArCCN(Me)CEt](\mu\text{-}H)$ (**6a,b**; Ar = Ph, Tol) were obtained in 30–40% yield. Compound **6a** was characterized structurally by a single-crystal X-ray diffraction analysis. An ORTEP drawing of the molecular structure of **6a** is shown in Figure 4. Final atomic positional parameters are listed in Table XII. Selected interatomic distances and angles are listed in Tables XIII and XIV. The molecule consists of a triangular cluster of three osmium atoms with eight linear terminal carbonyl ligands. The PMe$_2$Ph ligand is coordinated to Os(1), and one hydride ligand, H (located and refined crystallographically), δ = −15.71 ppm, bridges the Os(1)–Os(3) metal–metal bond. An EtCN(Me)CC-

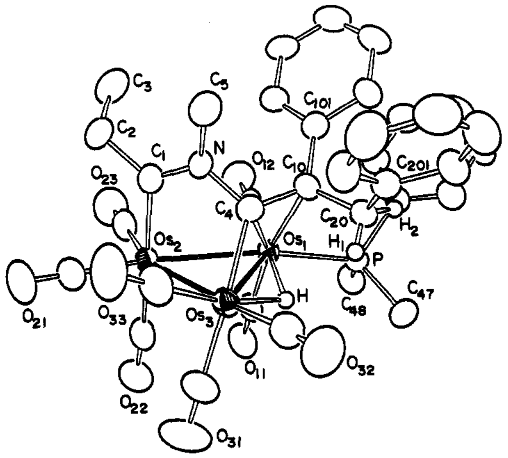

Figure 4. ORTEP diagram of $Os_3(CO)_8(PMe_2Ph)[\mu_3\text{-}PhH_2C(Ph)CCN(Me)CEt](\mu\text{-}H)$ (**6a**), showing 50% probability thermal ellipsoids.

Table XII. Positional Parameters and *B*(eq) Values for 6a

atom	*x*	*y*	*z*	*B*(eq), Å^2
Os(1)	0.177044 (20)	0.296063 (18)	0.503254 (12)	2.23 (1)
Os(2)	0.12670 (02)	0.208044 (20)	0.629048 (13)	2.61 (1)
Os(3)	0.30041 (02)	0.33065 (02)	0.634883 (13)	2.71 (1)
P	0.17963 (15)	0.38417 (13)	0.40071 (08)	2.68 (7)
O(11)	−0.0230 (05)	0.4005 (04)	0.5184 (03)	5.0 (3)
O(12)	0.0375 (05)	0.1531 (04)	0.4240 (03)	5.1 (3)
O(21)	0.1429 (05)	0.1462 (04)	0.7789 (03)	5.6 (3)
O(22)	−0.0279 (05)	0.3539 (04)	0.6676 (03)	5.4 (3)
O(23)	−0.0528 (05)	0.814 (05)	0.5722 (03)	5.7 (3)
O(31)	0.1819 (05)	0.4648 (05)	0.7167 (03)	7.2 (4)
O(32)	0.4944 (05)	0.4530 (05)	0.6454 (03)	6.5 (4)
O(33)	0.3857 (05)	0.2165 (05)	0.7615 (03)	6.0 (3)
O(100)	1.0000	0.055 (03)	1/4	17 (1)
N	0.3218 (04)	0.1366 (04)	0.5826 (03)	2.7 (2)
C(1)	0.2417 (06)	0.1112 (05)	0.6144 (03)	2.9 (3)
C(2)	0.2413 (06)	0.0140 (05)	0.6400 (04)	3.6 (3)
C(3)	0.2047 (08)	−0.0514 (06)	0.5817 (04)	5.5 (5)
C(4)	0.3259 (05)	0.2311 (05)	0.5595 (03)	2.6 (3)
C(5)	0.4196 (06)	0.0831 (06)	0.5844 (04)	3.9 (4)
C(10)	0.3509 (05)	0.2454 (05)	0.4911 (03)	2.4 (3)
C(11)	0.0514 (06)	0.3583 (05)	0.5135 (03)	3.2 (3)
C(12)	0.0951 (06)	0.2054 (05)	0.4539 (03)	3.2 (3)
C(20)	0.4219 (05)	0.3261 (05)	0.4803 (04)	2.7 (3)
C(21)	0.1380 (06)	0.1704 (05)	0.7223 (04)	3.7 (4)
C(22)	0.0307 (06)	0.3023 (06)	0.6507 (04)	3.7 (4)
C(23)	0.0141 (06)	0.1295 (06)	0.5914 (03)	3.5 (4)
C(31)	0.2276 (06)	0.4155 (06)	0.6872 (04)	4.4 (4)
C(32)	0.4218 (06)	0.4070 (06)	0.6378 (04)	4.0 (4)
C(33)	0.3523 (06)	0.2611 (06)	0.7139 (04)	4.0 (4)
C(41)	0.2336 (06)	0.3338 (05)	0.3268 (03)	3.1 (3)
C(42)	0.3156 (06)	0.3729 (06)	0.2980 (04)	4.0 (4)
C(43)	0.3502 (07)	0.3330 (07)	0.2391 (04)	5.0 (5)
C(44)	0.3030 (09)	0.2574 (08)	0.2104 (04)	6.1 (5)
C(45)	0.2210 (08)	0.2183 (06)	0.2401 (04)	5.6 (5)
C(46)	0.1872 (07)	0.2552 (06)	0.2976 (04)	4.4 (4)
C(47)	0.2386 (06)	0.4956 (05)	0.4116 (04)	3.7 (3)
C(48)	0.0462 (06)	0.4110 (06)	0.3586 (04)	3.9 (4)
C(101)	0.3540 (05)	0.1703 (05)	0.4389 (03)	2.8 (3)
C(102)	0.4249 (06)	0.1726 (05)	0.3898 (03)	3.4 (3)
C(103)	0.4286 (06)	0.1040 (06)	0.3417 (04)	4.0 (4)
C(104)	0.3615 (07)	0.0322 (06)	0.3392 (04)	4.4 (4)
C(105)	0.2912 (06)	0.0262 (05)	0.3876 (04)	3.8 (4)
C(106)	0.2882 (06)	0.0946 (05)	0.4358 (03)	3.3 (3)
C(201)	0.5413 (05)	0.3094 (05)	0.4991 (03)	2.8 (3)
C(202)	0.6102 (06)	0.3383 (06)	0.4534 (04)	3.8 (4)
C(203)	0.7182 (06)	0.3208 (06)	0.4674 (04)	4.8 (4)
C(204)	0.7578 (06)	0.2743 (06)	0.5273 (05)	4.6 (4)
C(205)	0.6935 (06)	0.2497 (06)	0.5730 (04)	4.7 (4)
C(206)	0.5848 (06)	0.2674 (06)	0.5595 (04)	3.9 (4)

Table XIII. Intramolecular Distances for 6a[a]

Os(1)–Os(2)	2.9103 (5)	Os(3)–C(33)	1.883 (8)
Os(1)–Os(3)	2.8443 (7)	Os(3)–H	1.74 (7)
Os(1)–P	2.377 (2)	P–C(41)	1.830 (7)
Os(1)–C(4)	2.263 (6)	P–C(47)	1.808 (8)
Os(1)–C(10)	2.380 (6)	P–C(48)	1.822 (7)
Os(1)–C(11)	1.880 (8)	N–C(1)	1.318 (8)
Os(1)–C(12)	1.873 (8)	N–C(4)	1.468 (9)
Os(1)–H	1.74 (8)	N–C(5)	1.473 (9)
Os(2)–Os(3)	2.8491 (7)	C(1)–C(2)	1.52 (1)
Os(2)–C(1)	2.095 (7)	C(2)–C(3)	1.51 (1)
Os(2)–C(21)	1.875 (7)	C(4)–C(10)	1.419 (9)
Os(2)–C(22)	1.937 (9)	C(10)–C(20)	1.53 (1)
Os(2)–C(23)	1.908 (8)	C(10)–C(101)	1.51 (1)
Os(3)–C(4)	2.129 (7)	C(20)–C(201)	1.53 (1)
Os(3)–C(31)	1.929 (9)	C–O(av)	1.14 (1)
Os(3)–C(32)	1.908 (9)	C(Ph)–C(av)	1.38 (1)

[a] Distances are in angstroms. Estimated standard deviations in the least significant figure are given in parentheses.

Table XIV. Intramolecular Bond Angles for 6a[a]

Os(2)–Os(1)–Os(3)	59.34 (2)	Os(2)–Os(3)–C(32)	176.7 (2)
Os(2)–Os(1)–P	166.79 (5)	Os(2)–Os(3)–C(33)	82.4 (2)
Os(2)–Os(1)–C(4)	71.2 (2)	C(4)–Os(3)–C(31)	160.0 (3)
Os(2)–Os(1)–C(10)	105.1 (2)	C(4)–Os(3)–C(32)	103.1 (3)
Os(2)–Os(1)–C(11)	80.7 (2)	C(4)–Os(3)–C(33)	96.3 (3)
Os(2)–Os(1)–C(12)	86.3 (2)	Os(1)–P–C(41)	118.8 (2)
Os(3)–Os(1)–P	125.34 (5)	Os(1)–P–C(47)	117.0 (2)
Os(3)–Os(1)–C(4)	47.6 (2)	Os(1)–P–C(48)	111.7 (2)
Os(3)–Os(1)–C(10)	75.0 (1)	C(41)–P–C(47)	105.4 (3)
Os(3)–Os(1)–C(11)	100.9 (2)	C(41)–P–C(48)	99.7 (3)
Os(3)–Os(1)–C(12)	141.5 (2)	C(47)–P–C(48)	101.6 (4)
P–Os(1)–C(4)	121.6 (2)	C(1)–N–C(4)	118.5 (6)
P–Os(1)–C(10)	88.1 (2)	C(1)–N–C(5)	123.0 (6)
P–Os(1)–C(11)	86.2 (2)	C(4)–N–C(5)	116.7 (5)
P–Os(1)–C(12)	92.2 (2)	Os(2)–C(1)–N	118.0 (5)
C(4)–Os(1)–C(10)	35.5 (2)	Os(2)–C(1)–C(2)	124.5 (5)
C(4)–Os(1)–C(11)	145.6 (2)	N–C(1)–C(2)	117.4 (6)
C(4)–Os(1)–C(12)	108.1 (3)	C(1)–C(2)–C(3)	112.1 (6)
Os(1)–Os(2)–Os(3)	59.18 (2)	Os(1)–C(4)–Os(3)	80.7 (2)
Os(1)–Os(2)–C(1)	87.2 (2)	Os(1)–C(4)–N	119.0 (4)
Os(1)–Os(2)–C(21)	160.4 (2)	Os(1)–C(4)–C(10)	76.8 (4)
Os(1)–Os(2)–C(22)	94.6 (2)	Os(3)–C(4)–N	115.5 (4)
Os(1)–Os(2)–C(23)	101.2 (2)	Os(3)–C(4)–C(10)	127.7 (5)
Os(3)–Os(2)–C(1)	83.4 (2)	N–C(4)–C(10)	116.7 (6)
Os(3)–Os(2)–C(21)	101.3 (2)	Os(1)–C(10)–C(4)	67.7 (3)
Os(3)–Os(2)–C(22)	92.6 (2)	Os(1)–C(10)–C(20)	110.2 (4)
Os(3)–Os(2)–C(23)	159.9 (2)	Os(1)–C(10)–C(101)	114.3 (4)
C(1)–Os(2)–C(21)	88.1 (3)	C(4)–C(10)–C(20)	117.3 (6)
C(1)–Os(2)–C(22)	174.0 (3)	C(4)–C(10)–C(101)	123.1 (6)
C(1)–Os(2)–C(23)	92.0 (3)	C(20)–C(10)–C(101)	114.2 (5)
Os(1)–Os(3)–Os(2)	61.48 (2)	C(10)–C(20)–C(201)	115.4 (6)
Os(1)–Os(3)–C(4)	51.7 (2)	P–C(41)–C(42)	122.4 (6)
Os(1)–Os(3)–C(31)	109.9 (2)	P–C(41)–C(46)	118.3 (6)
Os(1)–Os(3)–C(32)	118.4 (2)	Os(1)–H–Os(3)	110 (4)
Os(1)–Os(3)–C(33)	135.7 (2)	O–C(av)–Os	176 (1)
Os(2)–Os(3)–C(4)	74.2 (2)	C(Ph)–C(av)–C	120 (1)
Os(2)–Os(3)–C(31)	90.3 (2)		

[a] Angles are in degrees. Estimated standard deviations in the least significant figure are given in parentheses.

(Ph)CH$_2$Ph ligand bridges the face of the cluster. C(1) is a terminal carbene center as observed in **1**, **3a**, **4a**, and **5b**. C(4) bridges the Os(1)–Os(3) bond, and C(10) is coordinated to Os(1), but unlike **5b**, carbon C(20) is a phenyl-substituted methyl group that is not bonded to a metal atom. Both hydrogen atoms on C(20) were located and refined crystallographically. These hydrogen atoms are diastereotopic and appear in the ^{1}H NMR spectrum as an AB quartet, δ = 3.54 and 2.98 ppm, $^2J_{HH}$ = 14.5 Hz.

Scheme I

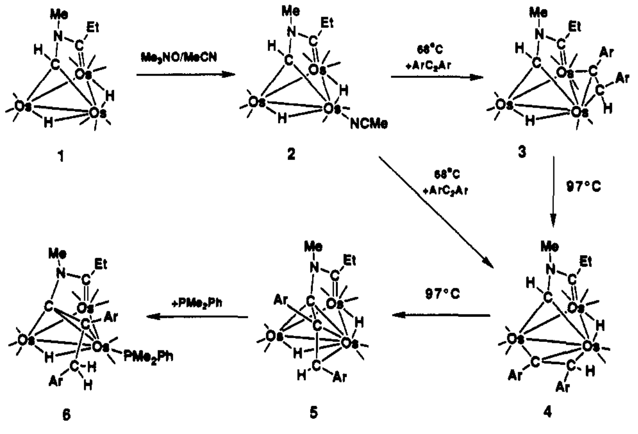

Discussion

A summary of the reactions and products obtained in this study is shown in Scheme I. By treatment of **1** with Me$_3$NO we have obtained the lightly stabilized acetonitrile derivative **2**. Compound **2** reacts with diarylalkynes, Ar = Ph or Tol, by substitution of the MeCN ligand and insertion into the metal hydrogen bonds to yield the isomeric products **3a,b** and **4a,b**, which contain bridging σ–π-coordinated diarylalkenyl ligands with a cis stereochemistry. The insertion of alkynes into the metal–hydrogen bonds of osmium cluster complexes is a well-established process.[7] The greatest difference between the isomers is the relative location of the bridging alkenyl group. In **4a**,**b** it bridges the same metal–metal bond that is bridged by the bridging carbene center. In **3a**,**b** it bridges one of the adjacent metal–metal bonds. The compounds **3a**,**b** can be converted to **4a**,**b** at 97 °C but not at an appreciable rate under the original reaction conditions, 68 °C. Therefore, it is believed that they are formed by competing insertion processes involving the two different hydride ligands in the original reaction. Also, the compounds **4a**,**b** do not return to **3a**,**b** when heated, indicating that they are the thermodynamically favored isomers. The compounds **4a**,**b** are, however, isomerized to yet another species, **5a**,**b**, at 97 °C in a process that involves the coupling of one the carbon atoms of the alkenyl ligand to the carbon atom of the bridging carbene by the formation of a carbon–carbon bond. The hydrogen atom that was originally bonded to the bridging carbene carbon was shifted to the metal atoms to become a bridging hydride ligand. There are a number of reports of the coupling of alkynes to bridging alkylidene ligands.[8] We recently reported an example of the coupling of the alkyne HC_2CO_2Me to a bridging *secondary* aminocarbene ligand that resulted in the elimination of the carbene hydrogen atom and hydride ligand from the metal atoms (eq 1).[9] It is believed that the compounds **4a**,**b** are the immediate precursors to **5a**,**b**, but this was not proven in this study.

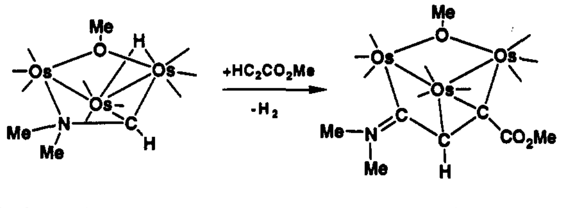

(1)

When the compounds **5a**,**b** were treated with PMe_2Ph, the PMe_2Ph was added to one of the osmium atoms and induced a shift of one of the hydride ligands to the aryl-substituted carbon atom that contained the hydrogen atom from the first insertion reaction. This occurs presumably by a reductive elimination process, but the mechanism of the transformation was not established. The result is the formation of an aryl-substituted methyl group. A variety of C–H-forming reductive elimination transformations have been observed in metal cluster complexes.[10] In a recent study, we have obtained evidence that indicates that carbon–hydrogen bond formation involving hydride ligand transfer can also occur by the process of deprotonation/reprotonation.[11]

Our results show that the bridging hydride ligands are the most reactive sites toward alkynes introduced to the complex **2**. The σ–π-coordinated alkenyl ligands show a strong preference for coupling to the bridging carbene center. We have found no evidence for reaction of the ethyl-substituted terminal carbene center with these alkynes. Certain nucleophiles (e.g. PMe_2Ph) can promote carbon–hydrogen bond formation between the hydride ligands and π-coordinated hydrocarbon ligands.

The bridging carbene center in compound **1** was formed by a series of CH activation transformations on one of the *N*-methyl groups of a terminally coordinated ethyl(dimethylamino)carbene ligand of the complex $Os_3(CO)_{11}[C(Et)NMe_2]$.[4] The activation of alkyl groups on the heteroatoms of carbene ligands is not easily accomplished in mononuclear metal–carbene complexes.[2] In this study we have demonstrated that the transformed methyl group can be functionalized by coupling to groupings derived from diarylalkynes. It seems reasonable to expect that the facile multicenter activation of the alkyl groups on carbene ligands in cluster complexes may serve as a general route for the functionalization of carbene ligands at these sites.

Acknowledgment. These studies were supported by the U.S. Department of Energy under Grant No. DE-FG09-84ER13296.

Supplementary Material Available: For all of the structural analyses, tables of hydrogen atom parameters and anisotropic thermal parameters (17 pages); tables of structure factor amplitudes (91 pages). Ordering information is given on any current masthead page.

---

[8] Herrmann, W. A. *Adv. Organomet. Chem.* **1982**, *20*, 159 and references therein.

[9] Adams, R. D.; Babin, J. E. *Organometallics* **1988**, *7*, 2300.

[10] Keister, J. B. *Polyhedron* **1988**, *7*, 847. (b) Ziller, J. W.; Bower, D. K.; Dalton, D. M.; Keister, J. B.; Churchill, M. R. *Organometallics* **1989**, *8*, 492.

[11] Adams, R. D.; Pompeo, M. P.; Tanner, J. T. *Organometallics* **1991**, *10*, 1068.